

Understanding quantum-box resonant-tunneling spectroscopy: Fine structure at Fermi-level crossings

Garnett W. Bryant*

McDonnell Douglas Research Laboratories, P.O. Box 516, St. Louis, Missouri 63166-0516

(Received 10 October 1990; revised manuscript received 24 January 1991)

We present calculations of the resonant-tunneling current through low-energy states (sharp resonances) confined in quantum-box nanostructures. We determine how the fine structure in the current provides a spectroscopy for these box states. Resonant tunneling produces fine structure when the box states are resonant with the emitter Fermi level. The results agree qualitatively with the observations of Reed *et al.*

Reed *et al.*^{1,2} and Tarucha *et al.*³ have used resonant-tunneling spectroscopy to probe electron states confined in zero-dimensional quantum boxes. Resonant-tunneling spectroscopy should be a *quantitative* spectroscopy for confined states in these structures because the single-particle states of isolated nanostructures (nA currents are obtained for individual nanostructures¹⁻³) can be probed directly by resonant-tunneling. The semiconductor nanostructures were fabricated from two-dimensional resonant-tunneling (2DRT) structures by laterally confining motion in the contact regions, the two barriers, and the quantum well. The laterally confined contacts are the quantum wires which connect to the quantum box. Quantum-box resonant tunneling (QBRT) measured at high temperatures and for large boxes is similar to 2DRT. Fine structure superimposed on a 2DRT-like current-voltage characteristic [see Fig. 1(a)] was observed for resonant tunneling through small boxes at low temperature ($T \sim 1-4$ K). This fine structure has been attributed to the discrete density of confined box states.¹⁻³

A quantitative resonant-tunneling spectroscopy for boxes requires an accurate model for the box states to determine which states participate in the tunneling and a theory for the resonant transport to indicate how the fine structure is produced by the discrete states. Resonant tunneling can proceed through direct channels⁴⁻⁶ in which the lateral quantum state is conserved, analogous to the conservation of lateral momentum in 2DRT. Resonant tunneling can also proceed through indirect channels⁵ in which the lateral quantum state is not conserved. In 2DRT the transverse momentum (Landau level if a magnetic field is present) of the tunneling state is conserved unless scattering by interface roughness, impurities, or phonons⁷⁻¹² couples the different transverse channels. In QBRT intrinsic variations in the lateral confinement of the structure can couple different transverse channels during tunneling without need for other scattering mechanisms.⁵ The lateral charge depletion from the sidewalls is shallower in the heavily doped contacts than in the lightly doped barriers and well of the box structure.¹⁻³ Thus the lateral confinement is weaker in the contacts than in the well. Carriers can tunnel through a box level in any lateral state which couples to

the emitter lateral subband by scattering from the spatial variation of the lateral confinement.⁵ For QBRT one must account for intrinsic indirect channels which do not occur in 2DRT.

Reed *et al.*¹ originally attributed the observed QBRT to tunneling through lateral sublevels derived from the well first excited state. Figure 1(b) shows the flat-band profile along the axis of the nanostructure—consisting of

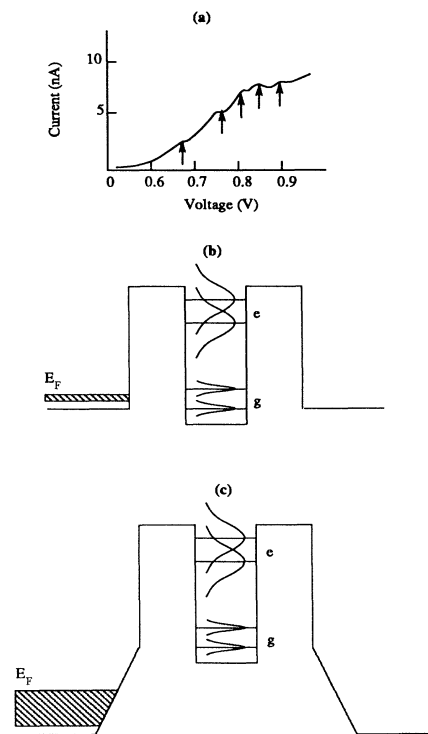


FIG. 1. (a) Low-temperature ($T \sim 1.0$ K) current-voltage characteristics of an isolated quantum-box nanostructure. (b) On-axis flat-band profile of a quantum-box nanostructure. Lateral states derived from the well ground (g) and first excited (e) state and the width of the resonances are indicated. (c) On-axis band profile when charge depletion is accounted for. The distribution of filled emitter states is indicated.

emitter, barrier, well, barrier, and drain—and the states trapped in the box. If the bands are flat at zero bias as shown in Fig. 1(b), then this identification of the well excited state as the tunneling channel must be made to explain why an applied bias of 600 meV was needed to initiate the resonant tunneling. The energies of the excited states are close to the top of the confining barriers, so the excited states are broad resonances.

Several initial calculations of QBRT (Refs. 4–6) have been done, but the experiments of Reed *et al.* have been modeled only in Ref. 5. In Ref. 5 resonant tunneling through excited states which are broad resonances was specifically modeled. A phenomenological band profile with flat bands, as in Fig. 1(b), was used to model the band profile along the axis of the nanostructure. The lateral confinement was modeled by harmonic potentials. The indirect channels were modeled phenomenologically by assuming that the coupling of different lateral states occurs only at barrier-contact and barrier-well interfaces and that the coupling can be described by a single, adjustable parameter which is the overlap between the lateral state on one side of the interface and the lateral state with the same quantum number on the other side of the interface.

For resonant tunneling through broad resonances, both direct and indirect channels produced fine structure in the calculated⁵ current-voltage characteristic but only if extreme assumptions were made about the lateral confinement in the GaAs contacts. Since the observed fine structure is split by roughly 50 meV, the lateral states should be split by about 25 meV, which is consistent with estimates¹ made for the lateral confinement energies. When the contact lateral confinement energies were assumed to be similar to the lateral confinement energies in the box, fine structure in the calculated current-voltage characteristics was not observable (see Fig. 3 of Ref. 5). In this case the tunneling resonance is broad, and the fine structure is further broadened by the distribution of filled emitter states, which is comparable to the box level spacing. Due to this additional broadening no fine structure is detectable. Observable fine structure in the calculated current-voltage characteristics was only found for the case in which the distribution of occupied emitter states was very narrow [as shown schematically in Fig. 1(b)]. The observation of several fine-structure peaks in the current implies that several emitter lateral subbands are occupied. Thus a narrow distribution of occupied emitter states can occur only if the emitter lateral confinement energies are small. In Ref. 5 we found that the calculated fine structure was observable when the emitter lateral confinement energy was ~ 1 meV. This is an extreme choice for this energy.

Recently Reed *et al.*² have developed an accurate model for the charge depletion and the confined states in their nanostructure. They find a large band bending [as shown in Fig. 1(c)] in the lightly doped region of the contact near the barriers. This large band bending, which is not present in two-dimensional double-barrier structures, is due to the lateral charge depletion. They find the barriers and well are 350 meV higher in energy when charge depletion is accounted for than in the flat-band case. For

that reason, one must assign the well ground state as the tunneling channel. The lateral sublevels derived from this well ground state should be sharp resonances. In this paper we recalculate the current-voltage characteristics to model the experiment of Reed *et al.* by use of a band profile, as in Fig. 1(c), which includes the band bending so that the resonant-tunneling channels are sharp resonances. We determine how information about the box states is revealed in quantum-box resonant tunneling when the box states are sharp resonances rather than broad resonances. We show that fine structure in the calculated current is observable for models of the nanostructure based on realistic parameters describing the structure when the resonances are sharp. Extreme choices for the emitter lateral confinement are *not* required to produce observable fine structure for tunneling through sharp resonances. We show that the fine structure occurs when the box states are resonant with the emitter *Fermi level* rather than the band edges of the emitter lateral subbands. In 2DRT the peaks do occur when the well states are resonant with the emitter conduction-band edge. Thus the peak structure in 2DRT and the fine structure in QBRT are qualitatively different. This insight must be included to develop a quantitative QBRT spectroscopy. Finally we show that indirect as well as direct channels will produce observable fine structure when the box states are sharp resonances.

The following qualitative model shows how tunneling through box states which are sharp resonances produces fine structure. As in 2DRT, QBRT through a particular box state occurs when the box state is resonant with the occupied source-contact states. In QBRT each contact lateral subband is a one-dimensional band of states. Each occupied contact lateral subband that is resonant with a box state and can couple to that box state during tunneling will provide two electrons (one for each spin) for tunneling at each applied bias. The dominant contribution to the current comes from direct tunneling channels that conserve the lateral quantum numbers of the tunneling state. For a direct channel through a sharp resonance, the current from an occupied source lateral subband has a step increase at the bias where the box state with the same lateral quantum numbers is resonant with the emitter Fermi level and a step decrease when the box state is resonant with the band edge for that subband. The current from a given subband is independent of bias (except for the effects of the transmission coefficient) between these limits (see Fig. 2). These discrete changes in current produce the fine structure. The step heights are proportional to the number of degenerate emitter subbands which contribute to the tunneling.

Direct-channel fine structure is produced by the step increases. For weak lateral confinement, these step increases merge into the linear rise of current with increasing bias seen in 2DRT. The voltage separation between adjacent steps is twice the splitting between adjacent box lateral levels (provided that the bias is applied symmetrically to the structure) and independent of the contact level spacings. A large total current analogous to the peak in 2DRT occurs when all the occupied emitter subbands contribute. When the lateral level spacings in the box

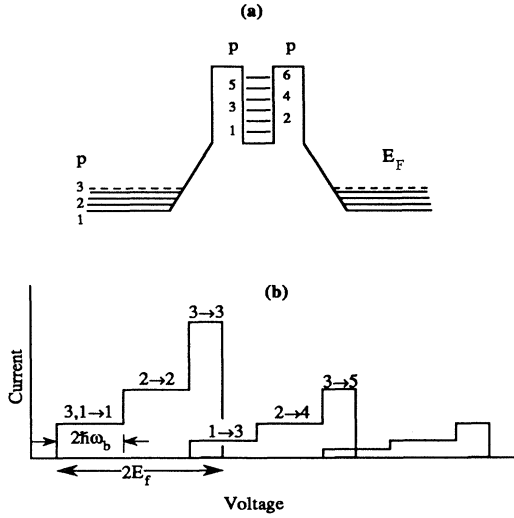


FIG. 2. (a) Contact lateral subbands and box states with level spacing $\hbar\omega_b$ for a nanostructure at zero bias; p is the lateral-state index. (b) Resonant-tunneling current for an emitter with three occupied subbands. Contributions from direct emitter-to-well ($p \rightarrow p$) and level-mixing ($p \rightarrow q$) channels are shown.

match the contact lateral level spacings, as assumed in Fig. 2 and as should occur approximately for quantum-box nanostructures, the band-edge crossings for the lateral levels will occur at the same bias. A sharp decrease in tunneling occurs because the box lateral subbands are simultaneously resonant with the corresponding emitter subband band edges. In practice, the resonances become broader as the applied bias increases and the sharp decrease is broadened away. Direct-channel fine structure is produced only by the step increases in current at Fermi-level crossings. These qualitative features are observed by Reed *et al.*^{1,2} (see Fig. 1). If the lateral level spacings in the box do not match the spacings in the emitter, fine structure from the step decreases should occur because the current from different subbands will turn off at different biases. However, because the resonances broaden as bias increases, the step decreases are too weak to produce fine structure.

The structure investigated by Reed *et al.* is nominally cylindrically symmetric and the lateral confining potential in each region is effectively parabolic. Successive lateral subbands, labeled by index p [see Fig. 2(a)], are equally spaced in energy. Each subband has well-defined transverse (x and y) parity. Only lateral states with the same transverse parity can couple by subband mixing. Direct-channel tunneling produces the $p \rightarrow p$ fine structure shown in Fig. 2. Additional fine structure due to tunneling from contact state p through box state q coupled by level mixing ($p \rightarrow q$ where $p - q$ is even when parity is conserved) occurs at higher applied bias (see Fig. 2).

When the tunneling channels are broad resonances,⁵ no clear interpretation of the fine structure as Fermi-level or band-edge crossings is possible. Fine structure is only observable if the distribution of filled emitter states is narrow. In that case the Fermi-level and band-edge cross-

ings are effectively simultaneous.

We confirm this qualitative insight by performing calculations for the multichannel tunneling current for zero-temperature single-particle resonant tunneling through the structure investigated by Reed *et al.*^{1,2} We use the same theory as used in Ref. 5. In Ref. 5 the on-axis band profile shown in Fig. 1(b) was used to model broad resonances. In this paper we use a phenomenological band profile, as shown in Fig. 1(c), which more accurately models the realistic band profiles determined by Reed *et al.*² to investigate resonant tunneling through sharp resonances. In our simplified model the lateral confining potential and energy levels are modeled by harmonic-oscillator states. We assume, as in Ref. 5, that these states change due to spatial variation in the lateral confinement only at the barrier interfaces. Level mixing occurs at the barrier interfaces to ensure that wavefunction boundary conditions at the interfaces are satisfied.

We solve the effective-mass Schrödinger equation numerically for each region in the structure, apply the boundary conditions at each interface to account for lateral level mixing and transmission across the interface, and use the results to determine the transmission coefficient for transport across the entire structure. We determine the zero-temperature resonant-tunneling current because temperature broadening at low temperatures (1–4 K) is small compared to the lateral level spacing. The total current is

$$I = \frac{e}{\pi\hbar} \sum_n \int_{E_{sn}} dE \frac{T(E, n, V) m_s}{\hbar k} [f(E) - f(E + V)],$$

where f is the occupation factor, V is the applied bias, k is the wave vector of the incident electron in source subband n with energy $E > E_{sn}$, m_s is the effective mass in the source, and T is the transmission coefficient for resonant tunneling from source subband n . The sum is over occupied source subbands. The integral is over occupied states in each subband. The details of the theory are the same as in Ref. 5 and are described fully therein.

A complete set of lateral states should be used to implement the boundary conditions at each interface. In practice, a finite basis set of lateral states is used. While use of a phenomenological model of level mixing based on a limited basis set cannot provide quantitative results, use of the model can show the importance of level-mixing effects. In our model⁵ the four lowest-energy lateral states for each possible x, y parity are included. The overlap matrix, which connects lateral states in one region with lateral states in the adjoining region, must be unitary; otherwise, the calculated current is not conserved during tunneling. A single parameter β , which is the overlap integral connecting one-dimensional transverse (x or y) states with the same quantum number from adjacent regions, determines the unitary overlap matrix in our model. Lateral states in adjacent regions are identical and no level-mixing occurs when $\beta=1$. Level-mixing occurs for $\beta < 1$. We treat β as an adjustable parameter to demonstrate the level-mixing needed to produce additional fine structure for tunneling through

sharp resonances.

The QBRT fine structure calculated for the structure of Reed *et al.* is shown in Figs. 3 and 4. In our model of the on-axis band profile [Fig. 1(c)] the barriers are 4 nm wide, the well is 5 nm, and the band bending near the barrier causes a linear rise of 350 meV over a 5-nm region. The actual band bending occurs over a wider region.² However, numerical problems in the calculation of the transmission coefficients arise when we try to model the band bending over too wide a region. Our model should provide the correct qualitative insight because the important effect of the band bending is to provide sharp resonances as the tunneling channels. The contacts are GaAs with effective mass $0.067m_e$. The barriers are $\text{Al}_x\text{Ga}_{1-x}\text{As}$ with effective mass $0.0919m_e$ and band offset 0.187 eV. The well is $\text{In}_x\text{Ga}_{1-x}\text{As}$ with effective mass $0.064m_e$ and band offset -0.051 eV. These parameters are similar to those used in Ref. 5. To produce results which best model the splitting of the fine structure observed in the experiments, we choose a box lateral level splitting $\hbar\omega_b$ of 26 meV. If the sidewall-depletion potential is the same in each region, then the level splitting scales as the square root of the effective mass. We use this scaling to choose level splittings in the barriers and contacts. Other more extreme choices for the contact level splitting could be made, as made in Ref. 5, but we have not tested these choices in detail in this work. For the results presented here, we assume that 50% of the bias drop is applied across the barriers and well and the remaining drop occurs across the lightly doped accumulation regions in the contacts adjacent to the barriers [see Fig. 1(c)]. For this model of the bias drop, the calculated current has the correct magnitude. For a smaller (larger)

percent of bias drop across the barriers and well, the fine structure is sharper (broader) and the current is larger (smaller). Results will be presented elsewhere to show how the tunneling depends on the details of the band bending, level splitting, applied bias drop, subband filling, etc.

Figure 3 shows the QBRT when only direct channels contribute. At least five contact lateral subbands must be occupied ($E_F \geq 5\hbar\omega_c$ where E_F is the Fermi energy relative to the emitter band edge and $\hbar\omega_c$ is the contact lateral level splitting) for the direct channels to produce all of the fine structure. Figure 3 shows the contribution from the five available channels when $E_F = 5.3\hbar\omega_c$. The step increase when a box state crosses the Fermi level is seen in the individual contributions and produces fine structure in the total current. The step decreases, which occur in the individual contributions when box levels are resonant with the band edge, are weak because the transmission resonances weaken with increasing bias. The step decreases do not produce fine structure in the total current. Fine structure due to step decreases is not seen in any of our calculations, even when box and contact lateral level splittings are different. Figure 3 shows that step increases can produce all five fine-structure peaks provided $E_F \sim 6\hbar\omega_c$.

Reed *et al.*² calculate a box lateral level splitting of 40 meV for their band profile model. This level splitting is too large to explain fine structure split by 50 mV, but might explain the 80-mV splitting between the two peaks at lowest bias. Reed *et al.*² also predict that only three contact lateral subbands are occupied. However, inclusion of level mixing can explain both the 80-mV splitting between the first two peaks,¹³ even when the levels are split by only 26 mV, and the appearance of more fine structure than the number of occupied bands. Figure 4

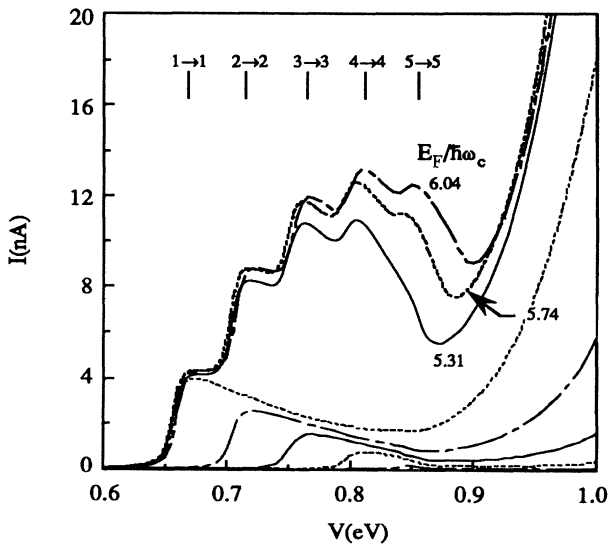


FIG. 3. Fine structure in the total resonant-tunneling current calculated including only direct channels for $E_F = 5.31, 5.74,$ and $6.04\hbar\omega_c$. The lower set of curves shows the current from each occupied source subband when $E_F = 5.31\hbar\omega_c$. The onset of tunneling for each direct ($p \rightarrow p$) channel is indicated.

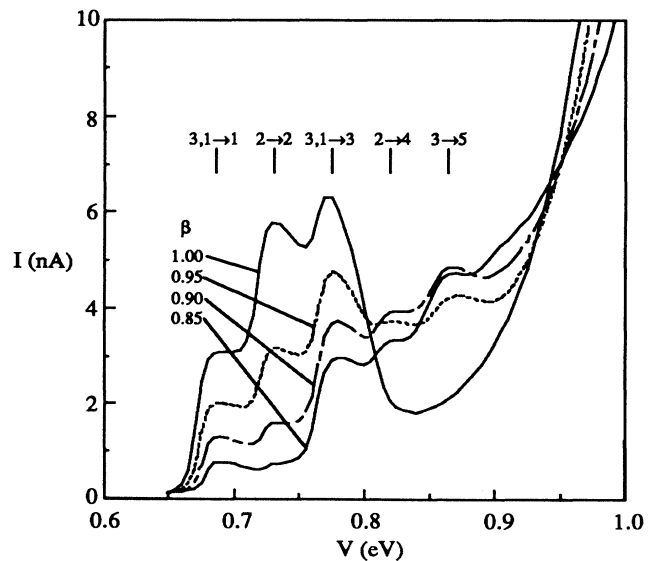


FIG. 4. Fine structure calculated including level mixing for $\beta = 1.0, 0.95, 0.9,$ and 0.85 for $E_F = 4\hbar\omega_c$. The channels are indicated.

shows the calculated fine structure as a function of level-mixing ($0.85 \leq \beta \leq 1.0$) for a structure with three occupied contact subbands ($E_F = 4\hbar\omega_c$). Additional fine structure at higher bias due to channels which are opened by level mixing is observable for $\beta \lesssim 0.95$. Level mixing also weakens resonant tunneling from direct channels. The second fine-structure peak, due to the direct channel for the lowest-energy lateral state with even x (y) and odd y (x) parity, is very weak for $\beta \lesssim 0.85$. Thus the large splitting between the first two observed peaks can be explained as a missing peak due to strong level-mixing effects. Similar conclusions about the possible effects of level mixing were made for tunneling through broad resonances.⁵

In summary, fine structure in QBRT through broad resonances is observable only if the distribution of emitter states is much narrower than the box-level spacing. Such a model is probably unrealistic. However, calculated fine structure for QBRT through sharp resonances is observable for realistic choices of the structure parameters. Direct and indirect channels can produce fine structure for tunneling through either type of resonance. However, a specific interpretation of the fine structure is possible if

the resonance is sharp. The fine structure due to a sharp resonance occurs when the bias brings a box state in resonance with the emitter Fermi level. This type of structure does not appear in 2DRT. The spacing of fine-structure peaks is determined by the box-level spacing and is independent of the emitter-level spacing. The fine structure is superimposed upon a main peak, which is analogous to the peak in 2DRT. Strong level mixing can explain missing fine-structure peaks and additional fine structure. Quantitative results depend critically on the model used: the band profile, lateral-level spacings, amount of level mixing, and subband filling. Developing a fully self-consistent model for band profiles for tunneling structures is still a difficult problem even for 2DRT.¹⁴ Full use of such a realistic band profile model in our theory of resonant transport in box structures should provide the theory needed for a quantitative QBRT spectroscopy.

This research was conducted under the McDonnell Douglas Independent Research and Development program.

*Present address: Applied Physics Branch, U.S. Army Harry Diamond Laboratory, Adelphi, MD 20783-1197.

¹M. A. Reed, J. N. Randall, R. J. Aggarwal, R. J. Matyi, T. M. Moore, and A. E. Wetsel, *Phys. Rev. Lett.* **60**, 535 (1988).

²M. A. Reed *et al.*, *Festkörperprobleme: Advances in Solid State Physics*, edited by U. Rössler (Vieweg, Braunschweig/Wiesbaden, 1989), Vol. 29.

³S. Tarucha, Y. Hirayama, T. Saku, and T. Kimura, *Phys. Rev. B* **41**, 5459 (1990).

⁴S. Y. Chou, E. Wolak, and J. S. Harris, Jr., *Appl. Phys. Lett.* **52**, 657 (1988).

⁵G. W. Bryant, *Phys. Rev. B* **39**, 3145 (1989).

⁶H. C. Liu and G. C. Aers, *Solid State Commun.* **67**, 1131 (1988); G. C. Aers and H. C. Liu, *ibid.* **73**, 19 (1990).

⁷J. Leo and A. H. MacDonald, *Phys. Rev. Lett.* **64**, 817 (1990).

⁸N. Wingreen, K. W. Jacobsen, and J. W. Wilkins, *Phys. Rev. Lett.* **61**, 1396 (1988).

⁹M. Jonson, *Phys. Rev. B* **39**, 5924 (1989).

¹⁰W. Cai, T. F. Zheng, P. Hu, B. Yudanin, and M. Lax, *Phys. Rev. Lett.* **63**, 418 (1989).

¹¹V. J. Goldman, D. C. Tsui, and J. E. Cunningham, *Phys. Rev. B* **36**, 7635 (1987).

¹²M. L. Leadbeater *et al.*, *Phys. Rev. B* **39**, 3438 (1989).

¹³M. Luban, J. H. Luscombe, M. A. Reed, and D. L. Pursey, *Appl. Phys. Lett.* **54**, 1997 (1989), proposed that the splitting between the first two levels would be larger than the splitting between other levels for an anharmonic confining potential.

¹⁴D. Landheer and G. C. Aers, *Superlatt. Microstruct.* **7**, 17 (1990).